

Date of publication xxxx 00, 0000, date of current version xxxx 00, 0000.

Digital Object Identifier ...

A High-Gain Leaky-Wave Antenna Using Resonant Cavity Structure with Unidirectional Frequency Scanning Capability for 5G Applications

A. GOUDARZI¹, M. M. HONARI², (Senior Member, IEEE), and R. MIRZAVAND³, (Senior Member, IEEE)

¹IWT lab, department of Mechanical Engineering, University of Alberta, Edmonton, Canada (e-mail: a.goudarz@ualberta.ca)

²Department of Electrical and Computer Engineering, University of Wisconsin-Madison, Madison, WI (e-mail: honarikalate@wisc.edu)

³IWT lab, department of Mechanical Engineering, University of Alberta, Edmonton, Canada (e-mail: mirzavan@ualberta.ca)

Corresponding author: R. Mirzavand (e-mail: mirzavan@ualberta.ca).

This work was supported by TELUS Communication Inc., The Natural Sciences and Engineering Research Council of Canada (NSERC), Alberta Innovate (AI), and CMC Microsystems.

ABSTRACT This paper presents a high-gain leaky-wave antenna based on a resonant cavity (RC) structure with the capability of unidirectional beam scanning over predefined frequencies and desired beam angles. Frequency scanning is achieved by implementing a properly-designed single-layer partially reflective surface (PRS) based on a simple ray tracing-based design procedure. In the proposed structure, two techniques are combined to make the beam scanning unidirectional. First, a metallic wall is placed at a proper distance from the radiator to suppress the antenna propagation at undesired directions. Second, a feed antenna with a tilted beam is designed as the main radiating element inside the cavity to radiate over desired beam angles. A prototype of the proposed antenna is fabricated and measured demonstrating a beam scanning from 12° to 46° over the frequency band from 25 to 31 GHz. Moreover, a maximum gain of 15.4 dBi is achieved at 26 GHz on the elevation plane with tilted angle of 22° . The proposed leaky-wave antenna is suitable for various wireless applications, in particular the 5th generation of cellular networks and small cell base station antenna (BSA) applications.

INDEX TERMS Base station antenna (BSA), leaky-wave, resonant cavity (RC), millimeter-wave, partially reflective surface (PRS), small cell, 5G antenna, unidirectional beam steering.

I. INTRODUCTION

Increasing demand for higher data rates and broader bandwidth has created an opportunity for next generation cellular communication systems, i.e., 5G, especially at millimeter frequencies around 28 GHz and 38 GHz [1]. However, the millimeter-wave (mmW) spectrum suffers from high loss and propagation issues such as interference, shadowing, and weaker penetration through objects. A suitable solution to mitigate this problem can be achieved by increasing the gain of the antenna while steering the antenna beam. Phased arrays have been considered as a proper configuration which can be used to improve the antenna gain and steer the main beam, simultaneously. Beam steering mechanism of phased arrays is based on applying phase differences between the antenna elements [2]. Although these antennas allow a high

speed scanning and high directivity, expensive and complicated phase shifter structures and antenna feed networks remain to be potential problems. Leaky-wave antennas (LWAs) are a qualified candidate to address the mmW spectrum concerns. LWAs have been attractive due to their frequency scanning feature, planar configuration, simple feeding network, and high-gain characteristics [3]–[9]. The mentioned features make LWAs attractive for future 5G small cell base station antennas (BSAs), and many works have addressed the 5G challenges based on the great features of LWAs.

Resonant cavity (RC) structures can significantly enhance the gain of a single antenna element [10]–[15]. Due to the leaky-mechanism of the RCAs, they are categorized as 2-D leaky-wave antennas. The RC antennas are composed of a partially reflective surface (PRS) placed at a proper distance

above a ground plane, surrounding a radiator or an array of radiators that feeds the entire structure [16], [17]. Multiple reflections inside the cavity between PRS and ground plane result in in-phase propagation leaking from the structure, which increases the antenna gain. There are many methods to achieve further gain enhancement. As such are using a PRS unit cell with positive reflection phase gradient, sharp resonance, or non-uniform structures in order to compensate for the non-uniform magnitude and phase distribution of the electric field over the antenna aperture [17]–[19]. There are several studies in the literature on beam steering of RCAs, some of which steer the antenna beam at a fixed frequency [20]–[31], while others do it over a frequency band [32]–[36] as leaky-wave antennas. Steering the antenna beam at a fixed frequency can be achieved by utilizing micro-electro-mechanical systems (MEMS) [20], PIN diodes [21], and varactors [22], [23]. In some recent studies [25]–[28], beam steering is achieved by mechanically rotating the structures, displacing the main radiating elements or creating phase differences between the radiating elements using power dividers. Such methods require complicated feeding networks or a complex control unit.

There are many works in the literature on the RCAs with frequency scanning capability [20], [32]–[37]. In conventional RC structures with a symmetric PRS fed by a main radiator at the center, either conical or broadside beams are achieved. There are only few studies on RC antennas with unidirectional beam steering. In [35], the unidirectional frequency scanning was achieved through using a periodic substrate integrated waveguide (SIW) LWA. In [36], by properly phasing the elements of a feeding system, the unidirectional beam steering was achieved with a low aperture efficiency of 6.9% at 18.5 GHz and the maximum gain of 17 dBi. In these studies, the main radiator mostly plays a significant role in obtaining the unidirectional beam steering. Using a well-designed PRS layer, however, might bring much more flexibility to the design for beam scanning over the desired frequency band and corresponding beam angles. In many applications, the range of both the operating frequencies and beam angles is predefined. Thus, this paper studies the design of a RCA with unidirectional frequency scanning capability over predefined frequency range within desired beam angles based on a systematic ray tracing-based design guideline with less computational process.

In this paper, a high-gain leaky-wave antenna with unidirectional beam scanning by varying frequency based on the RC structures is presented. The proposed antenna consists of a single-layer PRS, a main radiating element with a tilted beam, and a metallic wall. The PRS is theoretically designed based on a simple design procedure to simultaneously increase the antenna gain and steer the beam over predefined frequency range and corresponding desired beam angles. The feed antenna element is designed to have a tilted beam whose beamwidth covers the desired range of steering angles. A metallic wall is placed at a certain distance from the antenna structure to suppress the undesired propagation and create a

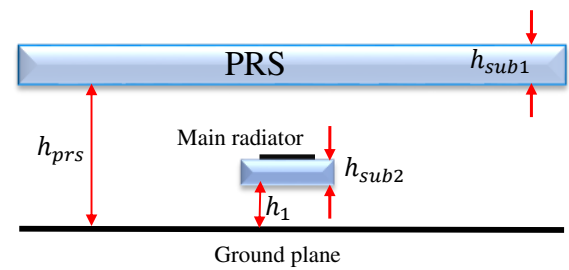


FIGURE 1. The configuration of a conventional RCA structure.

unidirectional radiation pattern. Finally, a prototype of the proposed antenna is fabricated and measured. The proposed antenna has the ability to steer the antenna beam from 12° to 46° over the frequency range from 25 GHz to 31 GHz, both defined as the predefined desired outputs. The results show a good agreement between simulation and measurement and confirm the reliability of the proposed antenna to be used in 5G small cell BSA.

The article is organized as follows: in Section II, a beam steering analysis is introduced. In Section III, a PRS with a performance closed to the analysis is designed. Moreover, the reflection behaviour of the designed PRS unit cell is studied. Section IV focuses on the design of the entire RCA structure including the main radiator. Besides, experiments are performed to validate the performance of the designed RCA prototype. Finally, conclusions are drawn in Section V.

II. BEAM STEERING ANALYSIS

The geometry of a conventional RC antenna, which consists of a main radiating element, a ground plane, and a PRS layer placed above the ground plane with an optimum distance of h_{prs} , is shown in Fig. 1. The PRS can be either a dielectric with a specific thickness or an array of patches with different patterns to make waves leak out [17]. There are various methods in order to analyze the RC mechanism such as ray tracing, transmission line (TL), LW, EBG, and the principle of reciprocity methods; among them, ray tracing is more popular [16]. Since ray tracing is a very straightforward and simple method, it is used in this paper for the design and analysis of the proposed RC antenna, which might be time consuming or complex by using the other methods.

In RC antennas, the radiation pattern is easily controlled by designing PRS structures such that they provide suitable magnitude and phase of reflection for different functionalities such as gain enhancement, polarization control, side lobe level reduction, etc. [17]. Based on the ray tracing method, and by controlling the amplitude and phase of the reflection coefficient in the unit-cell level, we can design an active antenna with beamforming capability at fixed frequencies or realize a leaky-wave antenna with beam scanning capability over a frequency range.

Here, the reflection coefficient of the PRS structure and the ground plane are given by $A_1 e^{-j\theta_{PRS}}$ and $A_2 e^{-j\theta_{Gnd}}$, where A_1 and A_2 are the magnitude of the reflection coefficients of

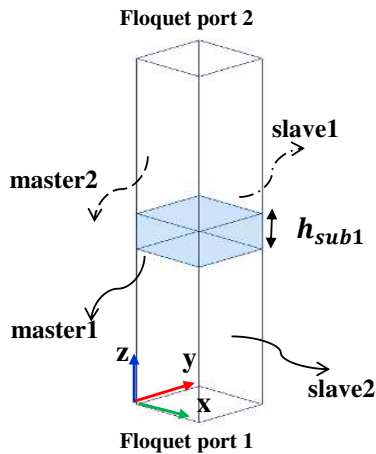


FIGURE 2. PRS unit cell boundary condition.

the PRS structure and the ground plane, respectively. Also, θ_{PRS} and θ_{Gnd} are assumed as the PRS and ground plane reflection phases, respectively. According to the ray tracing method, by utilizing the PRS layer, the antenna gain increases by [16]:

$$\Delta G = 10 \log \frac{1 + A_1}{1 - A_1} \quad (1)$$

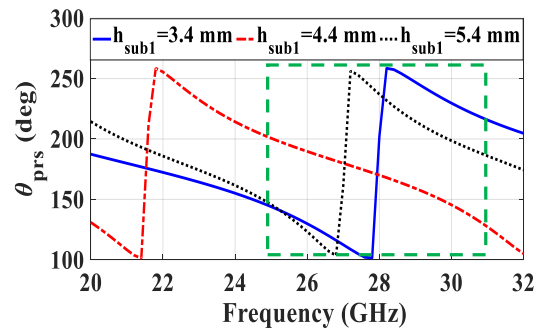
According to (1), increasing A_1 will elevate the antenna gain. For a perfect conductor ground plane with $\theta_{Gnd} = \pi$ and $A_2 = 1$, it can be shown that the resonance condition of RCAs is given by [16]:

$$\theta_{PRS}(f, \theta) + \theta_{Gnd} = 2N\pi + 2k \times h_{prs} \times \cos \theta \quad (2)$$

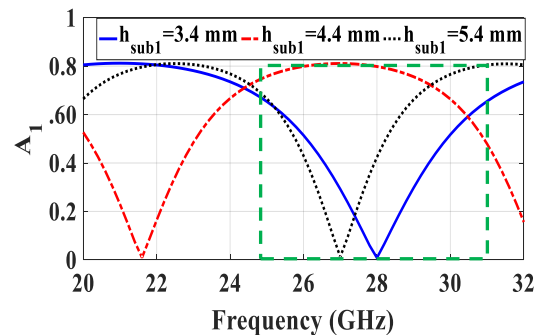
where $k = \frac{2\pi f}{c}$, c , and θ are the propagation constant, the speed of light, and the incident angle, respectively. $\theta_{PRS}(f, \theta)$ denotes the PRS reflection phase at the frequency f under the incident angle θ . It should be noted that h_{prs} can be calculated by (2) considering the reflection phase at a specific frequency and angle, then it can be used as a constant for the other frequencies and angles. The interesting point is that a leaky-wave relation with a high gain at $\theta_{PRS}(f, \theta)$ can be designed such that (2) is satisfied for a scanning range of frequency and angle θ . Under this circumstance, the antenna gain does not deteriorate over the operational bandwidth of the leaky-wave antenna.

The initial goal of this paper is steering the antenna beam from 10° to 45° over the frequency band of 25-31 GHz as desired beam angles and predefined frequency range, respectively. Consequently, a unit cell with a high reflection magnitude and a proper reflection phase is required over the desired bandwidth. In order to design the unit cell, it is necessary to determine the phase difference between the start (25 GHz) and end (31 GHz) frequencies of the desired band. Then, $\theta_{PRS}(f, \theta)$ is designed to have the beam steering from 10° at 25 GHz to 45° at 31 GHz.

For the design of the unit cell, the first step is to determine the value of h_{prs} . This can be calculated from (2) by having



(a)



(b)

FIGURE 3. Reflection characteristic of the proposed unit cell: (a) phase, and (b) magnitude of the unit cell for different values of h_{sub1} .

$\theta_{PRS}(f = 25 \text{ GHz}, \theta = 10^\circ)$ as the desired start frequency and beam angle. Then, the PRS needs to be designed such that its phase variation between the predefined start and end frequencies of the operating bandwidth satisfies the following equation:

$$\delta\theta = \theta_{PRS}(25 \text{ GHz}, 10^\circ) - \theta_{PRS}(31 \text{ GHz}, 45^\circ) \quad (3)$$

Hence, the reflection magnitude of the unit cell should be close to 1 and its phase difference at the edges of the frequency bandwidth needs to satisfy (3).

In the calculations, only the start and end frequencies along with their corresponding desired beam angles are considered for simplicity. The unit cell is then designed to obtain the desired reflection phase at start and end frequencies so that a beam scanning over desired angles at those predefined frequency range is achieved. This way, a systematic ray tracing-based design guideline is given as follows: First, based on the intended application, predefined ranges of sweeping frequency and corresponding beam angles are defined. Next, the PRS unit cell must be designed properly to provide the phase variations between start and end ranges. In fact, by substituting the start frequency and its associated angle in (2), and having an arbitrary reflection phase, obtained from an arbitrary PRS, the cavity height is calculated. After that, the PRS needs to catch the phase variations by satisfying (2) in other frequencies and angles. This phase variation is given

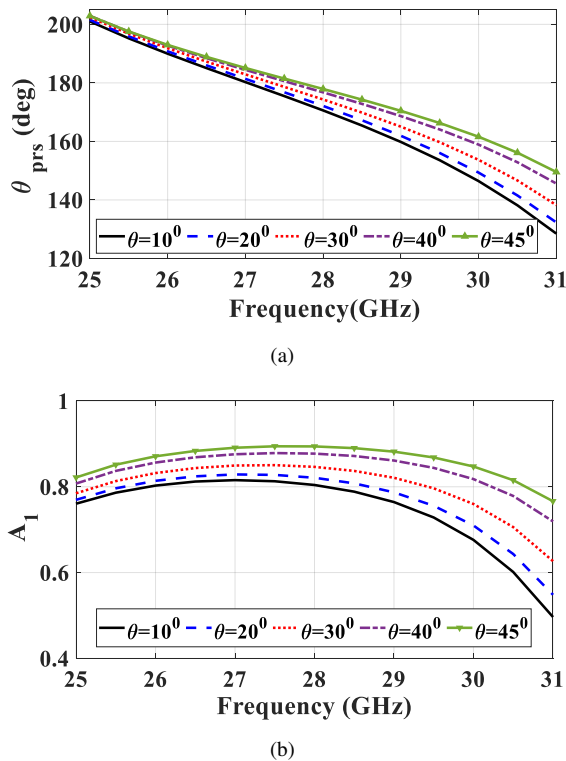


FIGURE 4. Reflection characteristic of the proposed unit cell with $h_{sub1} = 4.4$ mm: (a) phase, and (b) magnitude of the PRS unit cell under different incident wave angles.

in (3) for the required frequency and beam angle ranges in this paper.

In the next section, a single-layer unit cell that supports the beam steering over a predesigned frequency band is designed based on the above analysis.

III. PRS DESIGN

In this section, the design of a unit cell capable of steering the antenna beam over predetermined frequency range and desired beam angles is studied. Although any unit cell with metal and dielectric layers can be designed, a fully dielectric structure is designed here for simplicity. The Rogers TMM10i substrate with the thickness of h_{sub1} , relative permittivity of 9.8, and loss tangent of 0.002 is used as the PRS layer. The unit cell is simulated using Ansys HFSS with periodic boundary conditions and Floquet port excitation as shown in Fig. 2. First, designing a proper PRS, which is able to satisfy the phase difference estimated by (3) is of prime importance. Note that in fully dielectric unit cells, we have two key parameters, which are the thickness and permittivity of the dielectric in order to adjust the reflection phase and magnitude. The thickness of h_{sub1} has great impact on the proposed unit cell behaviour, which should be optimized to achieve the best performance. To have a deep insight into the impact of the substrate thickness on the reflection phase and magnitude, a parametric study is performed in Fig. 3. As shown, changing h_{sub1} affects both the phase and magnitude

of the unit cell. Based on Fig. 3(a), for $h_{sub1} = 4.4$ mm, the phase difference between the start and end frequencies is matched with the theoretical value of $\delta\theta = 42^\circ$, calculated by (3). Also, Fig. 3(b) shows that the proposed unit cell has a proper reflection magnitude over the desired frequency band of 25-31 GHz for $h_{sub1} = 4.4$ mm, while for the other values, the magnitude of the reflection coefficient has a sharp resonance or null over this frequency range. Thus, the optimum value of h_{sub1} is 4.4 mm due to its high reflection magnitude and desired phase variation over 25-31 GHz for achieving beam scanning.

For more investigation on the behaviour of the designed fully dielectric PRS unit cell with $h_{sub1} = 4.4$ mm, its reflection phase and magnitude for different incident wave angles versus frequency are demonstrated in Fig. 4. As shown, more variations are observed at higher frequencies. The reflection phase has the values of 200° and 150° at 25 GHz and 31 GHz, respectively, which are corresponding to the beam scanning angles of 10° at 25 GHz and 45° at 31 GHz, according to (2). The theoretical phase differences, i.e., $\delta\theta$, using (3), and the simulated phase difference based on Fig. 4(a) are around 42° and 50° , respectively, which are close together. This assures that the proposed unit cell is suitable to steer the antenna beam from 10° to 45° over the predetermined frequency band. Fig. 4(b) shows a high reflection magnitude around 0.8, demonstrating the ability of the proposed unit cell to increase the antenna gain over a wide frequency band from 25 to 31 GHz. Note that a metallo-dielectric unit cell might be designed to have much freedom to control the antenna radiation pattern. The same design procedure can be used to achieve the best initial design values. In fact, the unit cell reflection phase based on the predetermined frequencies and the desired beam angles needs to be obtained.

IV. RCA WITH STEERING BEAM

The proposed leaky-wave antenna based on an RC structure is depicted in Fig. 5. It consists of a feed antenna, a dielectric PRS, a metallic wall, and a ground plane. In order to have unidirectional beam scanning, two techniques are considered. The first one is to design a feed antenna with a tilted beam along with a metallic wall that suppresses undesired propagations and makes the radiation pattern unidirectional. The second step is the proper design of the PRS, which was discussed in the previous section to steer the beam by changing the frequency. To have a large scan angle with high gain, not only should the PRS phase be designed properly, but the feed antenna beamwidth needs to be wide. Consequently, both the PRS and feed antenna are required to be designed properly to have a large scanning angle with a high antenna gain.

A. ANTENNA FEED

This subsection focuses on designing a proper feed antenna inside the RC structure. It is aimed to design an antenna with a tilted beam for obtaining an unidirectional radiation beam, instead of a conical beam. The proposed feed is demonstrated

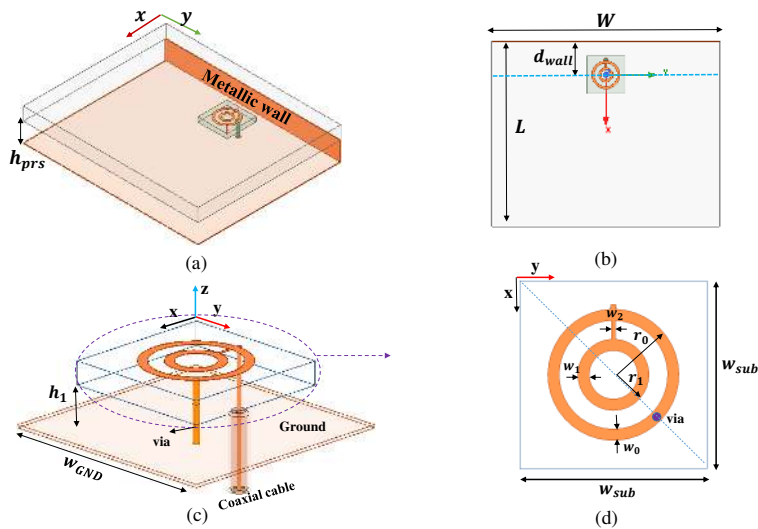


FIGURE 5. Proposed RCA structure: (a) perspective view, (b) top view, (c) perspective view, and (d) top view ($W = 60$, $L = 49$, $w_0 = 0.6$, $w_1 = 0.6$, $w_2 = 0.2$, $r_0 = 3.7$, $r_1 = 1.9$, $h_1 = 1$, $h_{sub1} = 4.4$, $d_{wall} = 9$, $w_{GND} = 30$, $w_{sub} = 10$, and $h_{prs} = 6.4$ all in mm).

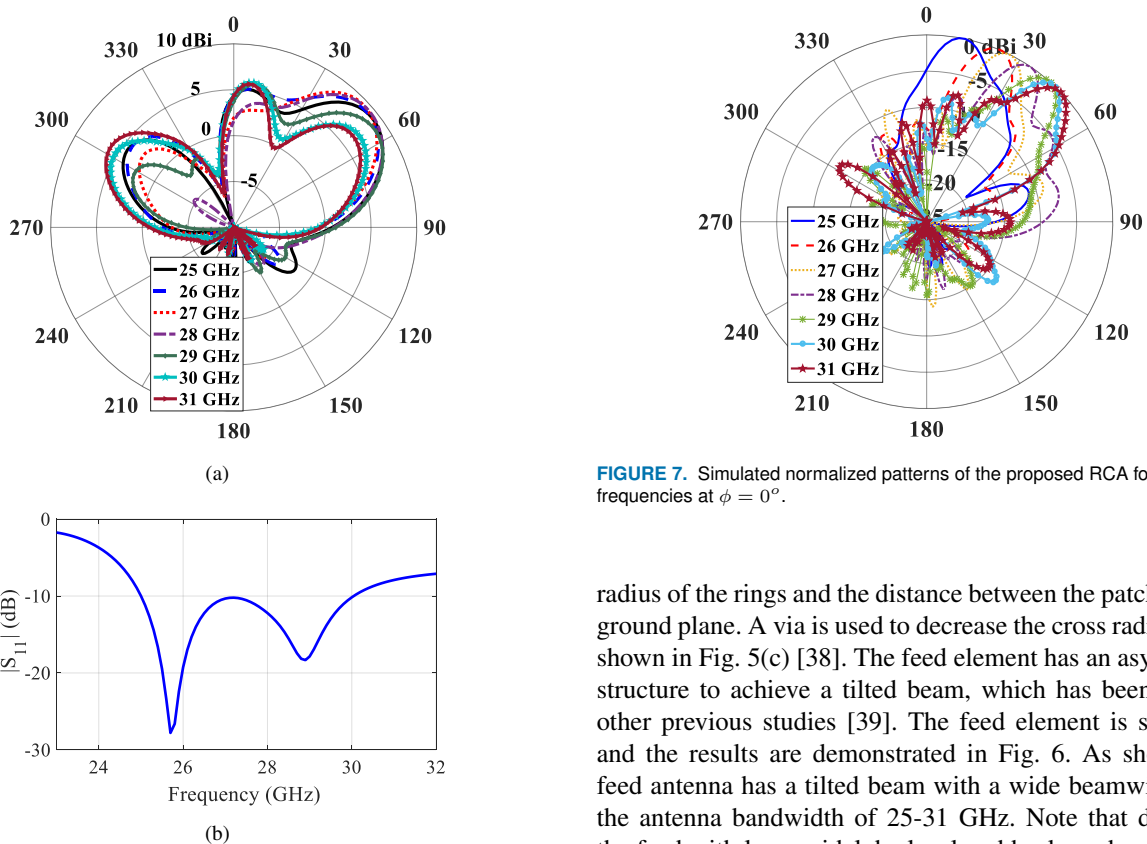


FIGURE 6. Simulation results of the feed antenna: (a) gain patterns at $\phi = 0^\circ$, and (b) S_{11} .

in Figs. 5(c) and 5(d). Two rings are printed on a Rogers TMM4 laminate with a thickness of $h_{sub2} = 1.524$ mm, relative dielectric constant of 4.5, and loss tangent of 0.002. The operating frequency band can be adjusted by changing the

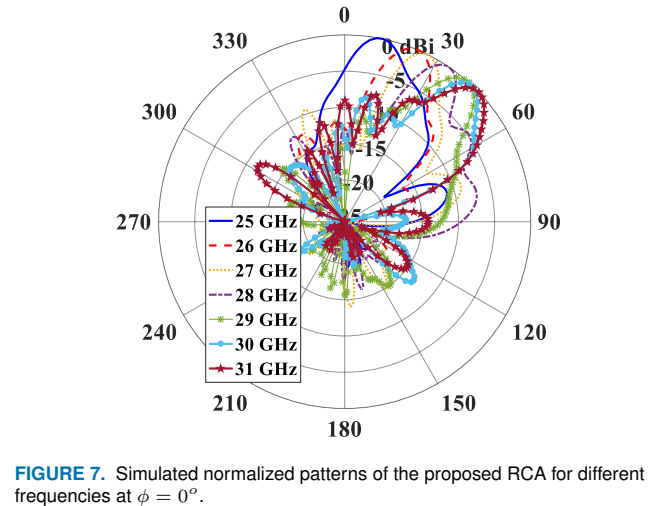


FIGURE 7. Simulated normalized patterns of the proposed RCA for different frequencies at $\phi = 0^\circ$.

radius of the rings and the distance between the patch and the ground plane. A via is used to decrease the cross radiation, as shown in Fig. 5(c) [38]. The feed element has an asymmetric structure to achieve a tilted beam, which has been used in other previous studies [39]. The feed element is simulated and the results are demonstrated in Fig. 6. As shown, the feed antenna has a tilted beam with a wide beamwidth over the antenna bandwidth of 25-31 GHz. Note that designing the feed with lower sidelobe level and backward radiation is desired. Therefore, in the final RCA structure, a metallic wall is also used to decrease such undesired radiation.

B. SIMULATION AND MEASUREMENT RESULTS

This subsection demonstrates the performance of the proposed leaky-wave antenna. The dielectric PRS is placed above the ground plane at a distance h_{prs} , as shown in Fig. 5(a). It is obvious that multi reflections in the cavity require

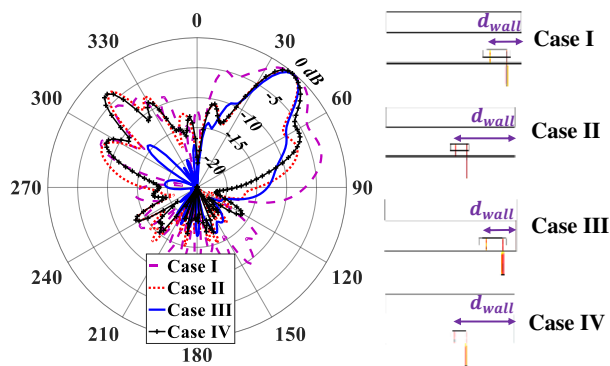


FIGURE 8. Effect of the metallic wall on the radiation pattern at 29 GHz ($d_{wall} = 9\text{ mm}$ for case I and case III and $d_{wall} = 30\text{ mm}$ for case II and case IV).

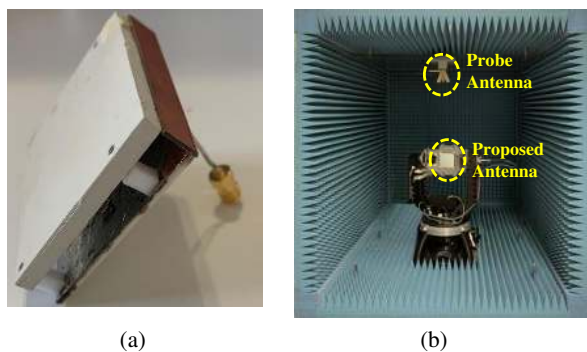


FIGURE 9. Fabricated antenna: (a) entire RC structure, and (b) antenna measurement setup.

bigger PRS structure as the scanning angle increases. Thus, the dimension of the PRS structure should be large enough to increase the antenna gain for the desired scanning angles. Therefore, optimizing the values of W and L is imperative. The simulated radiation patterns for different frequencies at $\phi = 0^\circ$ are shown in Fig. 7. As it is evident, the unidirectional beam scanning is achieved over the predefined frequency range of 25-31 GHz. It can be seen that the proposed RCA has a scan beam from 12° to 46° at 25 GHz and 31 GHz, respectively.

Fig. 8 is plotted to investigate the impact of the metallic wall on the antenna radiation pattern. As shown, four different cases are considered. For Case I and Case II, there is no metallic wall in the design, while in Case III and Case IV, the metallic wall is used with different distances from the feed antenna (d_{wall}). As can be seen from these four cases, the backward radiation can be suppressed to a certain degree by using a metallic wall with the optimized value of $d_{wall} = 9\text{ mm}$ (Case III).

To verify the performance of the designed RC antenna, the proposed structure is fabricated and measured with a DVTEST dbSafe enclosure using Signalshape® Near-field Antenna Measurement software. In fact, the near-field-to-far-field (NF-FF) transformation is performed to obtain the

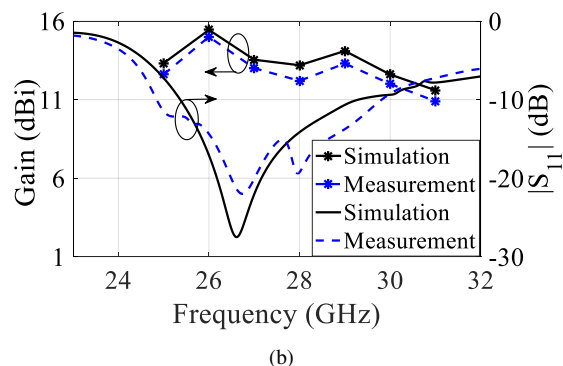
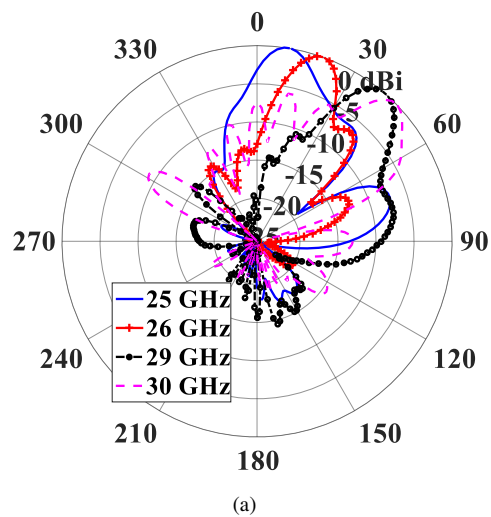


FIGURE 10. Results of the proposed RCA: (a) measured radiation patterns at $\phi = 0^\circ$, and (b) measured and simulated S_{11} and gain.

far-field radiation performance of the proposed antenna. A fabricated prototype of the proposed antenna and the measurement setup are shown in Fig.9. The measured radiation patterns for different frequencies at $\phi = 0^\circ$ are plotted in Fig. 10(a), which show the beam steering capability of the proposed antenna. The simulated and measured reflection coefficients and gain of the proposed RCA are in good agreement, as shown in Fig. 10(b). A maximum gain of 15.4 dBi is achieved at 26 GHz, which corresponds to the maximum aperture efficiency of 23.7%. The simulated and measured radiation patterns of the proposed antenna at 26 GHz are illustrated in Fig. 11. The slight differences between simulated and measured patterns are attributed to fabrication errors and alignments between the feed antenna and the PRS in the assembly process.

A comparison between the proposed RC antenna and other works in the literature is summarized in Table I. As seen, the proposed antenna in this paper shows a comparable leaky-wave performance with the works listed in Table I. In comparison with [20], the proposed antenna has higher antenna gain in addition to having an easier design approach. References [32] and [33] use multiple PRS layers to improve

TABLE 1. Comparison between the proposed antenna and different LWAs.

Ref	Realization Method	f_c (GHz)	Frequency sweep (GHz)	Scanning angle (deg)	Conical or unidirectional	Max-gain (dBi)	layer no.(#)	size (λ_c) ³
[20]	half phase gradient PRS with MEMS	10.6	9.9-11.3	12 to 50	Uni	13.5	1	$5.5 \times 5.5 \times 0.6$
[32]	spiraphase-type reflectarray	36.5	36.37-39.9	0 to 38	Conical	N.A	3	$12.2 \times 12.5 \times 0.2$
[33]	high-impedance surfaces	14	11-16	5 to 67	Uni	12.2	2	$9.2 \times 0.5 \times 1$
[35]	SIW LWA	11.85	9.1-14.6	-38 to 28	Uni	14.6	1	$5.37 \times 1.84 \times 0.67$
[36]	properly phasing the array feed	18	16-21	6 to 42	Uni	17	1	$8.43 \times 8.43 \times 0.2$
This work	PRS and tilted main radiator	28	25-31	12 to 46	Uni	15.4	1	$5.6 \times 4.5 \times 0.6$

f_c is the center frequency.
 λ_c is the wavelength at the center frequency.

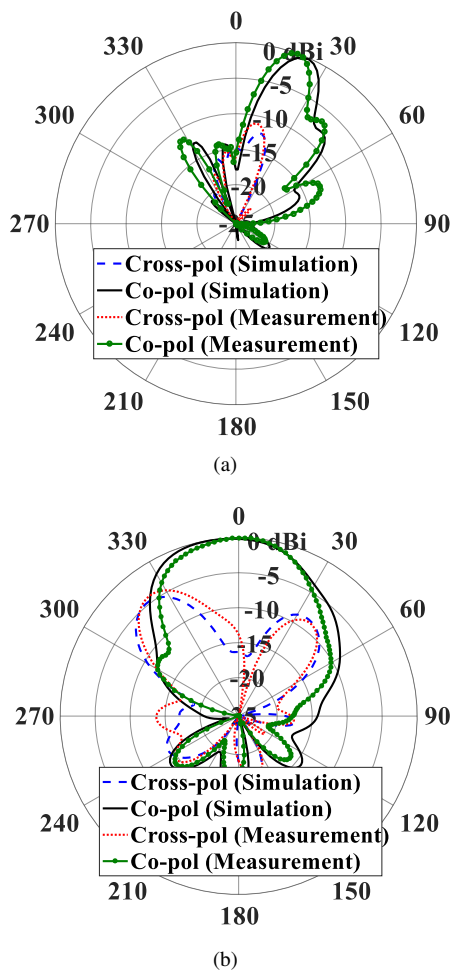


FIGURE 11. Measured and simulated radiation patterns at 26 GHz: (a) $\phi = 0^\circ$, and (b) $\theta = 24^\circ$ for simulation and $\theta = 22^\circ$ for measurement.

the radiation characteristics of the structure while this paper uses a single dielectric as PRS for simplicity. In [35], the PRS layer is only used for improving the radiation characteristics of the antenna and the beam scanning is performed by the main radiator. Also, in [35], the author used a PRS with a sharp reflection phase. This 180° jump in phase leads to a wide bandwidth. The main problem with such structures is the sudden gain drop at the resonant frequency of the PRS,

due to having a low reflection magnitude. In comparison with [36], the proposed antenna has smaller size and higher aperture efficiency. Moreover, the design in [36] needs to provide phasing for an array of feeds to steer the antenna beam. This makes the design and fabrication process more complex compared to our proposed antenna, where the PRS is responsible for beam steering.

V. CONCLUSION

In this paper, a leaky-wave antenna based on the RC structures with unidirectional beam scanning over the millimeter waves is presented. The proposed RCA consists of a main radiating element with tilted beam, a metallic wall, and a PRS layer. Utilizing a metallic wall and a main radiating element with a tilted beam are methods to make beam scanning unidirectional over the desired frequency band from 25 to 31 GHz. The PRS unit cell is designed based on a ray tracing-based design guideline so that the beam scanning by varying frequency is achieved, while the antenna gain is improved. A prototype of the antenna was fabricated and measured, and the results confirm the theoretical formula and the functionality of the proposed high-gain mmW leaky-wave antenna. A scan from 12° to 46° was achieved over the frequency band from 25 to 31 GHz. Moreover, a maximum gain of 15.4 dBi was achieved at 26 GHz on the elevation plane with tilted angle of 22° . The proposed antenna can be used in small cell BSAs while spatial frequency division is required.

...

REFERENCES

- [1] T. S. Rappaport, S. Sun, R. Mayzus, H. Zhao, Y. Azar, K. Wang, G. N. Wong, J. K. Schulz, M. Samimi, and F. Gutierrez, "Millimeter wave mobile communications for 5G cellular: It will work!," IEEE access, vol. 1, pp. 335–349, 2013.
- [2] R. J. Mailloux, Phased array antenna handbook. Artech house, 2017.
- [3] A. A. Oliner, D. R. Jackson, and J. Volakis, "Leaky-wave antennas," Antenna engineering handbook, vol. 4, p. 12, 2007.
- [4] D. K. Karmokar, Y. J. Guo, S.-L. Chen, and T. S. Bird, "Composite right/left-handed leaky-wave antennas for wide-angle beam scanning with flexibly chosen frequency range," IEEE Transactions on Antennas and Propagation, vol. 68, no. 1, pp. 100–110, 2020.
- [5] M. M. Honari, R. Mirzavand, J. Melzer, and P. Mousavi, "A new aperture antenna using substrate integrated waveguide corrugated structures for 5G

- applications," *IEEE Antennas and Wireless Propagation Letters*, vol. 16, pp. 254–257, 2017.
- [6] H. Jiang, K. Xu, Q. Zhang, Y. Yang, D. K. Karmokar, S. Chen, P. Zhao, G. Wang, and L. Peng, "Backward-to-forward wide-angle fast beam-scanning leaky-wave antenna with consistent gain," *IEEE Transactions on Antennas and Propagation*, vol. 69, no. 5, pp. 2987–2992, 2021.
- [7] M. U. Afzal, L. Matekovits, K. P. Esselle, and A. Lalbakhsh, "Beam-scanning antenna based on near-electric field phase transformation and refraction of electromagnetic wave through dielectric structures," *IEEE Access*, vol. 8, pp. 199242–199253, 2020.
- [8] M. M. Honari, A. Abdipour, and G. Moradi, "Aperture-coupled multi-layer broadband ring-patch antenna array," *IEICE Electronics Express*, vol. 9, no. 4, pp. 250–255, 2012.
- [9] M. Wang, H. F. Ma, H. C. Zhang, W. X. Tang, X. R. Zhang, and T. J. Cui, "Frequency-fixed beam-scanning leaky-wave antenna using electronically controllable corrugated microstrip line," *IEEE transactions on antennas and propagation*, vol. 66, no. 9, pp. 4449–4457, 2018.
- [10] C. Gu, S. Gao, B. S. Izquierdo, G. J. Gibbons, P. R. Young, E. A. Parker, F. Qin, G. Wen, Z. Cheng, Y. Geng, et al., "Wideband high-gain millimetre/submillimetre wave antenna using additive manufacturing," *IET Microwaves, Antennas & Propagation*, vol. 12, no. 11, pp. 1758–1764, 2018.
- [11] M. M. Honari, P. Mousavi, and K. Sarabandi, "Miniaturized-element frequency selective surface metamaterials: A solution to enhance radiation off of RFICs," *IEEE Transactions on Antennas and Propagation*, pp. 1–1, 2019.
- [12] M. M. Honari, R. Mirzavand, and P. Mousavi, "A high-gain planar surface plasmon wave antenna based on substrate integrated waveguide technology with size reduction," *IEEE Transactions on Antennas and Propagation*, vol. 66, pp. 2605–2609, May 2018.
- [13] A. Goudarzi, M. Movahhedi, M. M. Honari, H. Saghlatoon, R. Mirzavand, and P. Mousavi, "Wideband high-gain circularly polarized resonant cavity antenna with a thin complementary partially reflective surface," *IEEE Transactions on Antennas and Propagation*, pp. 1–6, 2020.
- [14] A. Goudarzi, M. Movahhedi, M. M. Honari, and P. Mousavi, "A wideband cp resonant cavity antenna with a self-complimentary partially reflective surface," 2020 IEEE AP-S Symposium on Antennas and Propagation, 2020.
- [15] A. Lalbakhsh, M. U. Afzal, K. P. Esselle, S. L. Smith, and B. A. Zeb, "Single-dielectric wideband partially reflecting surface with variable reflection components for realization of a compact high-gain resonant cavity antenna," *IEEE Transactions on Antennas and Propagation*, vol. 67, no. 3, pp. 1916–1921, 2019.
- [16] G. V. Trentini, "Partially reflecting sheet arrays," *IEEE Trans. Antennas Propag.*, vol. 4, no. 4, pp. 666–671, 1956.
- [17] A. Goudarzi, M. M. Honari, and R. Mirzavand, "Resonant cavity antennas for 5G communication systems: A review," *Electronics*, vol. 9, no. 7, p. 1080, 2020.
- [18] T. Hayat, M. U. Afzal, A. Lalbakhsh, and K. P. Esselle, "Additively manufactured perforated superstrate to improve directive radiation characteristics of electromagnetic source," *IEEE Access*, vol. 7, pp. 153445–153452, 2019.
- [19] A. Goudarzi, M. Movahhedi, M. M. Honari, and R. Mirzavand, "Design of a wideband single-layer partially reflective surface for a circularly-polarized resonant cavity antenna," *AEU - International Journal of Electronics and Communications*, vol. 129, p. 153535, 2021.
- [20] H. Moghadas, M. Daneshmand, and P. Mousavi, "Mems-tunable half phase gradient partially reflective surface for beam-shaping," *IEEE Transactions on Antennas and Propagation*, vol. 63, no. 1, pp. 369–373, 2014.
- [21] M. Li, S.-Q. Xiao, Z. Wang, and B.-Z. Wang, "Compact surface-wave assisted beam-steerable antenna based on his," *IEEE Transactions on Antennas and Propagation*, vol. 62, no. 7, pp. 3511–3519, 2014.
- [22] T. Debogović and J. Perruisseau-Carrier, "Array-fed partially reflective surface antenna with independent scanning and beamwidth dynamic control," *IEEE transactions on antennas and propagation*, vol. 62, no. 1, pp. 446–449, 2013.
- [23] R. Guzman-Quiros, J. L. Gomez-Tornero, A. R. Weily, and Y. J. Guo, "Electronically steerable 1-D fabry-perot leaky-wave antenna employing a tunable high impedance surface," *IEEE Transactions on Antennas and Propagation*, vol. 60, no. 11, pp. 5046–5055, 2012.
- [24] A. H. Naqvi and S. Lim, "A beam-steering antenna with a fluidically programmable metasurface," *IEEE Transactions on Antennas and Propagation*, vol. 67, no. 6, pp. 3704–3711, 2019.
- [25] M. U. Afzal and K. P. Esselle, "Steering the beam of medium-to-high gain antennas using near-field phase transformation," *IEEE Transactions on Antennas and Propagation*, vol. 65, no. 4, pp. 1680–1690, 2017.
- [26] T. Hongnara, S. Chaimool, P. Akkaraekthalin, and Y. Zhao, "Design of compact beam-steering antennas using a metasurface formed by uniform square rings," *IEEE Access*, vol. 6, pp. 9420–9429, 2018.
- [27] K. K. Katare, A. Biswas, and M. J. Akhtar, "Microwave beam steering of planar antennas by hybrid phase gradient metasurface structure under spherical wave illumination," *Journal of Applied Physics*, vol. 122, no. 23, p. 234901, 2017.
- [28] L. Ji, G. Fu, and S.-X. Gong, "Array-fed beam-scanning partially reflective surface (PRS) antenna," *Progress In Electromagnetics Research*, vol. 58, pp. 73–79, 2016.
- [29] K. K. Katare, S. Chandravanshi, A. Biswas, and M. J. Akhtar, "Beam-switching of fabry-perot cavity antenna using asymmetric reflection phase response of bianisotropic metasurface," *IET Microwaves, Antennas & Propagation*, vol. 13, no. 6, pp. 842–848, 2019.
- [30] L.-Y. Ji, Y. J. Guo, P.-Y. Qin, S.-X. Gong, and R. Mittra, "A reconfigurable partially reflective surface (PRS) antenna for beam steering," *IEEE Transactions on Antennas and Propagation*, vol. 63, no. 6, pp. 2387–2395, 2015.
- [31] M. U. Afzal, A. Lalbakhsh, and K. P. Esselle, "Electromagnetic-wave beam-scanning antenna using near-field rotatable graded-dielectric plates," *Journal of applied physics*, vol. 124, no. 23, p. 234901, 2018.
- [32] J. I. M.-L. . A. E. M. Daniel Seseña-Martinez, Jorge Rodriguez-Cuevas, "Spiraphase-type leaky-wave structure," *Journal of Electromagnetic Waves and Applications*, vol. 31, no. 6, pp. 561–576, 2017.
- [33] M. Garcia-Vigueras, J. L. Gomez-Tornero, G. Goussetis, A. R. Weily, and Y. J. Guo, "Enhancing frequency-scanning response of leaky-wave antennas using high-impedance surfaces," *IEEE Antennas and Wireless Propagation Letters*, vol. 10, pp. 7–10, 2011.
- [34] E. Abdo-Sánchez, M. Chen, A. Epstein, and G. V. Eleftheriades, "A leaky-wave antenna with controlled radiation using a bianisotropic huygens' metasurface," *IEEE Transactions on Antennas and Propagation*, vol. 67, no. 1, pp. 108–120, 2018.
- [35] W. Ma, W. Cao, S. Shi, Z. Zeng, and X. Yang, "Gain enhancement for circularly polarized SIW frequency beam scanning antenna using a phase-correcting grating cover," *IEEE Access*, vol. 7, pp. 52680–52688, 2019.
- [36] D. Comite, M. Kuznetsov, V. G.-G. Buendía, S. K. Podilchak, P. Baccarelli, P. Burghignoli, and A. Galli, "Directive 2-D beam steering by means of a multi-port radially periodic leaky-wave antenna," *IEEE Transactions on Antennas and Propagation*, 2020.
- [37] J. Zhan, F. Xu, S. Liu, S. Deng, L. Yang, and J. Qiang, "Frequency scanning fabry-perot cavity antenna with single 2D-varying partial reflecting surface," *IET Microwaves, Antennas & Propagation*, vol. 14, no. 11, pp. 1246–1252, 2020.
- [38] X. Zhang and L. Zhu, "Patch antennas with loading of a pair of shorting pins toward flexible impedance matching and low cross polarization," *IEEE Transactions on Antennas and Propagation*, vol. 64, no. 4, pp. 1226–1233, 2016.
- [39] W. Dale Ake, M. Pour, and A. Mehrabani, "Asymmetric half-bowtie antennas with tilted beam patterns," *IEEE Transactions on Antennas and Propagation*, vol. 67, no. 2, pp. 738–744, 2019.